JOURNAL OF GUIDANCE, CONTROL, AND DYNAMICS
Vol. 17, No. 6, November–December 1994

Deployment/Retrieval Control of Tethered Subsatellite Through an Optimal Path

Hironori A. Fujii* and Seiichi Anazawa†
Tokyo Metropolitan Institute of Technology, Hino, Tokyo 191, Japan

Development of a feedback control law to follow an optimal path is presented concerning the deployment/retrieval phase of a subsatellite connected to the Shuttle through a tether. The optimal path to be tracked is obtained numerically by solving a two-point boundary-value problem with inequality constraints on tether tension that is the control force, with fixed boundary conditions, and with an unspecified terminal time. The feedback control algorithm is designed using a Lyapunov function to asymptotically reduce the deviation of the actual trajectory from the optimal path. The Lyapunov function is defined to be positive definite and to be zero when the trajectory coincides simultaneously with the optimal path. The present method of control is simulated numerically, and the results show excellent controlled response of the tethered subsatellite system. A comparison of the present approach with the neighboring optimum feedback control is also presented and shows the superior performance of the tracking-type control using the Lyapunov function for large initial variations from the optimal path.

I. Introduction

TETHERED subsatellite systems have the potential of playing important roles in future space missions. Some of the applications are, for example, cargo transfer, assembly of space structures, generation of artificial gravity, release of artificial meteors, rendezvous procedure, and low-altitude science applications.[1–4] One future mission of the tethered subsatellite necessitates the process of deploying the tethered subsatellite from the Shuttle to access altitudes as low as 100–150 km. This mission is necessary since altitudes between 100 and 150 km are too high for balloons or research aircraft and too low for satellites in circular orbits. Control of the deployment/retrieval processes of the tethered subsatellite in this mission is essential in order to accomplish the mission objective.

This paper is concerned with the design of a control algorithm for the deployment/retrieval phase of the tethered subsatellite connected to the Shuttle. Various control laws have been proposed to date to complete the deployment/retrieval phase of the tethered subsatellite such as the tether tension control, the tether length rate control, and thrust-augmented torque control.[5–15] Rupp[16] investigated a control problem for deployment with a tension control law that is a linear function of tether length, its rate, and the commanded length. Feedback gains in the tension control law are determined by utilizing the natural frequency of the equations of motion. An optimal control law is presented based on an application of the linear regulator problem by Bainum and Kumar,[17] and the tension control law involving tether length, its rate, in-plane angle, its rate, and the commanded length is applied for the deployment/retrieval and stationkeeping phases. Among them a nonlinear tension control named the mission-function control is presented by Fujii et al.[18–20] using the concept of the Lyapunov function. The mission function control is also applicable to control distributed-parameter systems as shown by Junkins et al.[21] for the near-minimum-time control of slew maneuvers.

In this paper, the concept of an optimal path is presented for the deployment/retrieval of the tethered subsatellite, and the mission-function control is applied to the tracking-type control in order to follow the optimal path. Results of the numerical simulation show excellent controlled behavior of the tethered subsatellite system to confirm the effectiveness of the present control method.

Received June 5, 1993; revision received March 24, 1994; accepted for publication April 12, 1994.

*Professor, Department of Aerospace Engineering. Member AIAA.
†Graduate Student, Department of Aerospace Engineering.

II. Description of System

The system of the tethered subsatellite connected to the Shuttle is illustrated in Fig. 1. The center of attraction is denoted by P and the center of mass of the Shuttle by C. The orthogonal axes X, Y, and Z are defined along PC, along the orbital velocity vector, and along the orbital angular velocity vector, respectively, originating at C. The parameters m, l, Θ, and ϕ denote mass of the subsatellite, length of the tether, position angle of the subsatellite in the orbital plane (in-plane), and that in the out of plane, respectively.

In this study, the following assumptions are made:

1) The mass of the subsatellite is sufficiently small with respect to the mass of the Shuttle and C always remains in its nominal orbit.

2) The tether has no mass and thus its flexibility is ignored.

3) The only external force affecting the motion is the gravitational force caused by P. The orbit is circular with a radius R_0 and a constant angular velocity Ω.

4) The control force acts only along the tether through tension T, and no control force or energy dissipation exists for motion perpendicular to the tether line.

Under the above assumptions, the nondimensional equations of motion are obtained as follows:

$$\Lambda'' - \Lambda\phi'^2 - \Lambda\Theta'^2\cos^2\phi - 2\Lambda\Theta'\cos^2\phi - 3\Lambda\cos^2\Theta\cos^2\phi + \Lambda\sin^2\phi = -\hat{T} \tag{1a}$$

$$\Lambda\Theta''\cos\phi + 2\Lambda'\Theta'\cos\phi - 2\Lambda\Theta'\phi'\sin\phi + 2\Lambda'\cos\phi - 2\Lambda\phi'\sin\phi + 3\Lambda\sin\Theta\cos\Theta\cos\phi = 0 \tag{1b}$$

$$\Lambda\phi'' + 2\Lambda'\phi' + \Lambda\Theta'^2\sin\phi\cos\phi + 2\Lambda\Theta'\sin\phi\cos\phi + 3\Lambda\cos^2\Theta\sin\phi\cos\phi + \Lambda\sin\phi\cos\phi = 0 \tag{1c}$$

where $(\cdot)' = d(\cdot)/d\tilde{\tau}$, $\tilde{\tau} = \Omega t$, t is time, $\Lambda = l/|l(t=0) - l_m|$, l_m is the desired length for the deployment or retrieval, and $\hat{T} = T/[m\Omega^2|l(t=0) - l_m|]$ is the tension in nondimensional form.

Numerical simulations are presented for the case when the Shuttle is assumed to follow a circular orbit with a radius of 6600 km and orbital velocity 7.065×10^{-2} rad/min. The boundary conditions for calculating the optimal path for the deployment/retrieval are as follows (where t_f is the terminal time):

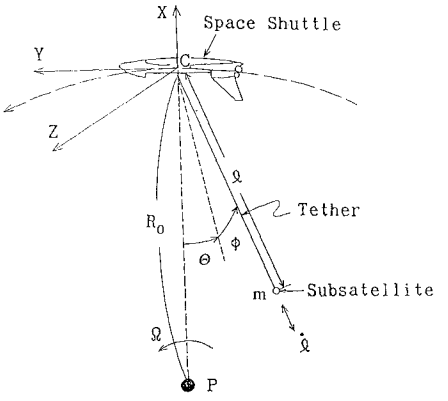

Fig. 1 Schematic representation of tethered satellite system.

For the deployment phase:

$$\begin{pmatrix} l_{t=0} \\ l'_{t=0} \\ \Theta_{t=0} \\ \Theta'_{t=0} \\ \phi_{t=0} \\ \phi'_{t=0} \end{pmatrix} = \begin{pmatrix} 1\text{ km} \\ 10\text{ m/s} \\ 0 \\ 0 \\ 0 \\ 0 \end{pmatrix} \qquad \begin{pmatrix} l_{t=t_f} \\ l'_{t=t_f} \\ \Theta_{t=t_f} \\ \Theta'_{t=t_f} \\ \phi_{t=t_f} \\ \phi'_{t=t_f} \end{pmatrix} = \begin{pmatrix} 100\text{ km} \\ 0\text{ m/s} \\ 0 \\ 0 \\ 0 \\ 0 \end{pmatrix} \tag{2}$$

For the retrieval phase:

$$\begin{pmatrix} l_{t=0} \\ l'_{t=0} \\ \Theta_{t=0} \\ \Theta'_{t=0} \\ \phi_{t=0} \\ \phi'_{t=0} \end{pmatrix} = \begin{pmatrix} 100\text{ km} \\ 0\text{ m/s} \\ 0 \\ 0 \\ 0 \\ 0 \end{pmatrix} \qquad \begin{pmatrix} l_{t=t_f} \\ l'_{t=t_f} \\ \Theta_{t=t_f} \\ \Theta'_{t=t_f} \\ \phi_{t=t_f} \\ \phi'_{t=t_f} \end{pmatrix} = \begin{pmatrix} 1\text{ km} \\ 0\text{ m/s} \\ 0 \\ 0 \\ 0 \\ 0 \end{pmatrix} \tag{3}$$

The initial velocity for the deployment phase is set to be 10 m/s due to a maximum velocity that is provided by the Shuttle.

III. Optimal Path

A. Optimal Path with Cost Index Minimum

The optimal path is presented in this paper in the sense that the time integral of squared tension in the reel mechanism is minimum. There are several solutions for different terminal times, as shown in Figs. 2a and 2b. Therefore, the terminal time is also optimized to decide an optimal path among them.

To obtain the optimal path of the subsatellite for the deployment/retrieval, nondimensional time is defined using an unknown terminal time t_f that is to be optimized:

$$\tau = \tilde{\tau}/t_f, \qquad 0 \le \tau \le 1 \tag{4}$$

Thus the problem can be treated as a problem with the terminal time fixed. Let us consider a problem to find control force $\hat{T}(\tau)$ to minimize the performance index

$$J = \tfrac{1}{2} t_f \int_0^1 (R\hat{T}^2 + Q\Theta^2)\, d\tau \tag{5}$$

with the inequality constraints

$$\hat{T}_{\min} \le \hat{T} \le \hat{T}_{\max}, \qquad \hat{T}_{\min} = 0.01, \qquad \hat{T}_{\max} = 4.0 \tag{6}$$

where R and Q are positive weighting coefficients. The inequality constraints of the nondimensional tension is introduced as in Eq. (6). The lower bound of the constraints is set since tether becomes slack if the tension is less than zero. The upper bound is also set since the tolerable tension is limited for the existing tether material whereas the value of the nondimensional tension is about 3.03 ($<\hat{T}_{\max}$) in the state of static equilibrium at the altitude of 100 km.

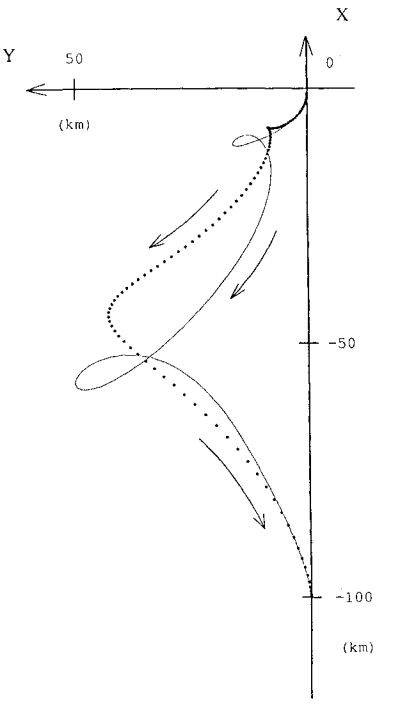

Fig. 2a Optimal paths for two different terminal times (deployment phase); · · · —terminal time is about 80 mins; —— —terminal time is about 71 mins.

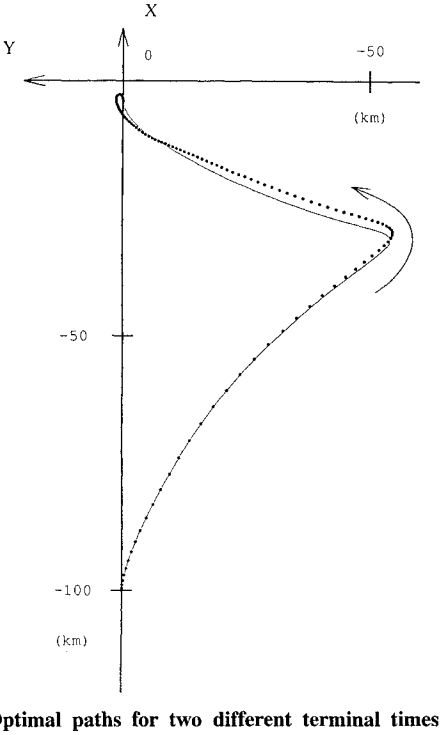

Fig. 2b Optimal paths for two different terminal times (retrieval phase); · · · —terminal time is about 71 mins; —— —terminal time is about 85 mins.

The motion of the system is described by Eqs. (1) with the initial boundary conditions $x(\tau = 0)$ and the constraining function $\varphi[x(\tau = 1)]$ of the terminal state as follows [where $x(\tau) = (\Lambda, \Lambda', \Theta, \Theta', \phi, \phi')$]:

$$x(0) = (\Lambda_0, \Lambda'_0, \Theta_0, \Theta'_0, \phi_0, \phi'_0) = \text{given}$$

$$\varphi[x(1)] = (\Lambda - \Lambda_{\tau=1}, \Lambda', \Theta, \Theta', \phi, \phi') = (0, 0, 0, 0, 0, 0) \tag{7}$$

The augmented performance index is written as

$$J^* = [\nu^t \varphi]_{\tau=1} + \int_0^1 \left[\tfrac{1}{2} t_f (R\hat{T}^2 + Q\Theta^2) + \lambda^t (t_f f - x')\right] d\tau \quad (8)$$

where $\lambda(\tau)$ and ν are the multiplier functions and multipliers, respectively.

The Euler-Lagrange equations then become as follows:

$$\lambda'' = -\frac{\partial H}{\partial x} \quad (9a)$$

$$\frac{\partial H}{\partial \hat{T}} = 0 \quad (9b)$$

$$x' = \frac{\partial H}{\partial \lambda} \quad (9c)$$

where H is the Hamiltonian defined as

$$H = t_f\left[\tfrac{1}{2}(R\hat{T}^2 + Q\Theta^2) + \lambda^t f\right] \quad (10)$$

The optimal condition for the control force [Eq. (9b)] is to be modified under the constraint of its inequality condition, Eq. (6). That is to say that the Hamiltonian is minimized by the optimal control force $T^*(\tau)$ under the constrained condition.

The boundary condition of the multiplier functions is obtained as follows:

$$\lambda^t(1) = \left[\nu^t \frac{\partial \varphi}{\partial x}\right]_{\tau=1} \quad (11)$$

The condition for the terminal time is defined as

$$\frac{\partial J^*}{\partial t_f} = 0 \quad (12)$$

Consequently, the problem is reduced to a two-point boundary-value problem that consists of the equations of the multiplier functions (9a) and the equations of motion (9c) with the boundary conditions (7) and (11). The optimal control tension $T^*(\tau)$ is not easily obtained analytically and is sought through numerical analysis employing the conjugate gradient method[22] and the multiplier method. The clipping-off method[23] is also employed to treat the present problem with the constrained control force.

B. Conjugate Gradient Method[22] and Clipping-Off Method[23]

The control force $\hat{T}(t)$ is considered to be an n-component vector for numerical analysis. The minimum value of J^* can be obtained through the numerical iteration of $\hat{T}$. Denoting the numbers of iteration by i, the $(i+1)$th iteration of $\hat{T}$ is calculated from the ith selection of $\hat{T}$:

$$\hat{T}_{i+1} = \hat{T}_i + \alpha_i s_i, \qquad s_{i+1} = -g_{i+1} + \beta_i s_i$$
$$\beta_i = |g_{i+1}|^2 / |g_i|^2 \quad (13)$$

where $\alpha_i = \min_\alpha J^*(\hat{T}_i + \alpha S_i)$ and $g_i = \partial J_i^* / \partial \hat{T}_i$.

In this study, since the control tension is constrained, s and β are defined by the clipping-off method as follows:

$$\beta_i = \begin{cases} \beta^0, & \beta^0 < \beta^m \\ \gamma \beta^m, & \beta^0 \geq \beta^m \\ 0, & I_2 = 0 \text{ or } I_3 = 0 \end{cases} \qquad (0 < \gamma < 1) \quad (14)$$

where

$$\beta^0 = I_1 / I_2 (I_2 \neq 0), \qquad \beta^m = I_1 / I_3 \qquad (I_3 \neq 0)$$

$$I_1 = \int_{U_i} \left(J^*_{\hat{T}_i}, J^*_{\hat{T}_i}\right) d\tau, \qquad I_2 = \int_{U_i} \left(J^*_{\hat{T}_{i-1}}, J^*_{\hat{T}_{i-1}}\right) d\tau$$

$$I_3 = \int_{U_i} \left(J^*_{\hat{T}_i}, s_{i-1}\right) d\tau$$

Consequently,

$$s_i(\tau) = \begin{cases} -J_{\hat{T}_i} + \beta_i s_{i-1}(t), & \tau \in U_i^* \\ -J_{\hat{T}_i}, & \tau \in S_i^* \end{cases} \quad (15)$$

where S^* denotes the event when the tension is saturated and U^* denotes the event when the tension is not saturated.

IV. Mission-Function Control

A. Control Along Optimal Path

Let the subscript t denote the state of the optimal path along the trajectory of equations of motion. The deployment/retrieval phase is controlled by a tracking-type control law to reduce the deviation of the actual trajectory from the optimal path. Tracking-type control is applied because a controlled motion with the optimal control tension $T^*(\tau)$ only does not trace the optimal path in the presence of inevitable state observation errors or parameter uncertainty of the system. Furthermore, even if a neighboring optimum feedback control,[24] which is obtained by linearizing Eqs. (7–11) around the optimal path and can stabilize small perturbations from the optimal path, is applied, the trajectory with the neighboring optimum feedback control does not trace the optimal path under the existence of a large deviation, as shown in Fig. 3. The control law presented in this paper is a feedback control algorithm using the mission-function control algorithm,[18–20] which is designed to stabilize asymptotically the deviation of the trajectory from the optimal path by generating a Lyapunov function called the mission function. The mission function is defined to be positive definite and to be zero when the trajectory coincides simultaneously with the optimal path.

The following mission function M_1 is applied for the tracking-type control:

$$M_1 = M_0^2 \quad (16a)$$

$$\begin{aligned} M_0 = {} & \tfrac{1}{2}\{a_1(\Lambda - \Lambda_t)^2 + b_1[(\Lambda' - \Lambda_t')^2 + (\Lambda\Theta' - \Lambda_t\Theta_t')^2 \\ & + 3(\Lambda \sin\Theta - \Lambda_t \sin\Theta_t)^2] + c_1(\Lambda\phi - \Lambda_t\phi_t)^2\} \\ & + b_1 \int_0^\tau (\Lambda_t\Lambda_t' - \Lambda\Lambda') \\ & \times \left[\Theta_t'(\Theta' - \Theta_t') - 3(\Theta - \Theta_t)\sin\Theta_t \cos\Theta_t\right] d\tau \\ & - c_1 \int_0^\tau (\Lambda\phi - \Lambda_t\phi_t)(\Lambda\phi' - \Lambda_t'\phi)\, d\tau \qquad (0 \leq \tau \leq 1) \end{aligned} \quad (16b)$$

where a_1, b_1, and c_1 are the positive weighting coefficients.

The optimal path is calculated with the terminal state fixed. The values of the terminal state in the optimal control are selected as

$$\Lambda_t = \Lambda_m, \qquad \Lambda_t' = \Theta_t = \Theta_t' = \phi_t = \phi_t' = 0 \quad (17)$$

where Λ_m is the nondimensional length at the objective state.

Using Eqs. (1), the nondimensional time derivative of the mission function is obtained along the trajectory of the system as follows:

$$\frac{dM_1}{d\tau} = -(\Lambda' - \Lambda_t')M_0\tilde{T}_1 + E \quad (18)$$

where

$$\begin{aligned} \hat{T}_1 = {} & \hat{T}_t + (a_1/b_1 + 3)(\Lambda - \Lambda_t) + c_1\phi(\Lambda\phi - \Lambda_t\phi_t) \\ & + (\Lambda + \Lambda_t)[\Theta_t'(\Theta' - \Theta_t') - 3(\Theta - \Theta_t)\sin\Theta_t\cos\Theta_t] \\ & + \tilde{T}_1/b_1 \qquad (0 \leq \tau \leq 1) \end{aligned} \quad (19)$$

and

$$\begin{aligned} E = {} & -3\Lambda\Lambda_t'\left\{\tfrac{1}{3}(\Theta' - \Theta_t')^2 + (\sin^2\Theta_t + \Theta_t'\sin\Theta_t\cos\Theta_t)\right. \\ & \left. \times (\Theta - \Theta_t)^2 - (\Theta - \Theta_t)(\Theta' - \Theta_t')\sin^2\Theta_t\right\} \end{aligned} \quad (20)$$

Here $\tilde{T}_1$ is the freely assignable part of $\tilde{T}_1$ and E is the error term with no definite sign.

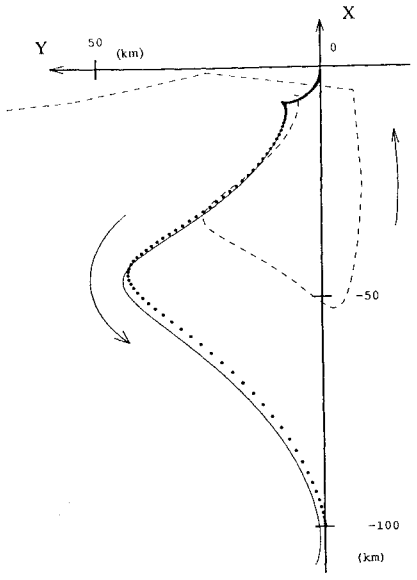

Fig. 3 Trajectory with a neighboring optimum feedback control. ··· —optimal path for the tethered subsatellite; a) —— —trajectory with the optimal control tension including a neighboring optimum feedback control and b) - - - —trajectory with the optimal control tension including a neighboring optimum feedback control; Initial conditions: a) $l = 1.1$ km, $l' = 10$ m/s, $\Theta = \Theta' = 0.0$ and b) $l = 1.1$ km, $l' = 10$ m/s, $\Theta = 0.1$, $\Theta' = 0.0$.

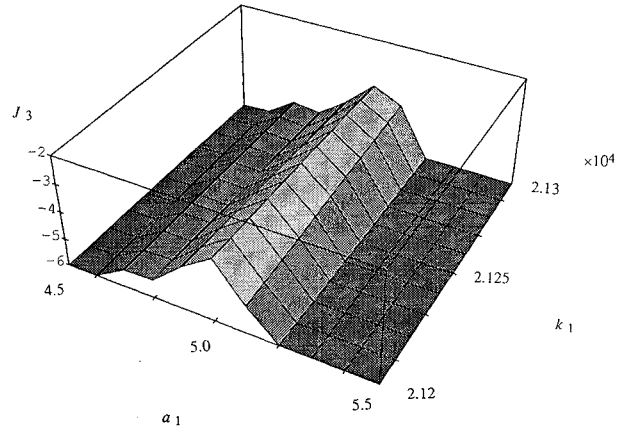

Fig. 4 Value of J_3 with respect to values of positive weighting coefficients a_1 and k_1 (retrieval phase).

Selection of $\tilde{T}_1$ in this case as

$$\tilde{T}_i = k_1(\Lambda' - \Lambda_t')M_0 \qquad (k_1 > 0) \tag{21}$$

gives the following representation of the time derivative of the mission function:

$$\frac{dM_1}{d\tau} = -k_1 M_0^2(\Lambda' - \Lambda_t')^2 + E \tag{22}$$

The time derivative of the mission function cannot be set perfectly to be negative definite due to the error term E. If the error of the rotational angle of the subsatellite from the optimal path is assumed to be sufficiently small and its terms higher than second order are neglected, the error term E vanishes. The following performance index is defined to select the values of the positive weighting coefficients a_1, k_1, and b_1 that can make the error of the rotational angle from the optimal path small and the error term E ignored:

$$J_3 = -\int_0^1 |\Theta - \Theta_t| \, d\tau \tag{23}$$

The coefficients are determined under the condition that the nondimensional tension $\hat{T}_1$ is not negative and less than $\hat{T}_{\max}$. Consequently, $\hat{T}_1$ is selected in this paper to be the control force. Figure 4 shows the variation for values of J_3 with respect to the values of the weighting coefficients a_1 and k_1 with the value of b_1 and the initial conditions fixed. It is apparent from this figure that the coefficients can be selected to improve the control performance by reducing the deviations of the rotational angle from the optimal path integrated for the time from 0 to 1.

B. Control After Terminal Time

Another type of mission function, M_2,[20] is applied to complete the given mission after the time period t_f and is defined as follows:

$$2M_2 = a_2(\Lambda - \Lambda_m)^2 + a_3\Lambda^2 + b_3\Lambda^2(\Theta^2 + 3\sin^2\Theta)$$
$$(\tau \geq 1) \tag{24}$$

where a_2, a_3, and b_3 are the positive weighting coefficients. As apparent from Eq. (24), the mission function M_2 is positive definite and zero at the objective state, Eq. (17).

The nondimensional time derivative of the mission function is obtained as

$$\frac{dM_2}{d\tau} = -\Lambda'\tilde{T}_2 \tag{25}$$

where

$$\hat{T}_2 = \Lambda(\Theta'^2 + 2\Theta' + 3\cos\Theta^2) + \frac{a_2}{a_3}(\Lambda - \Lambda_m)$$
$$+ \frac{b_2}{a_3}\Lambda[-\Theta'^2 + 3\sin\Theta^2 - 2\Theta'] + \frac{1}{a_2}\tilde{T}_2 \qquad (\tau \geq 1) \tag{26}$$

and $\tilde{T}_2$ is the freely assignable part of $\hat{T}_2$.

Selection of $\tilde{T}_2$ in this case as

$$\tilde{T}_2 = k_2\Lambda' \qquad (k_2 > 0) \tag{27}$$

gives the following representation of the time derivative of the mission function:

$$\frac{dM_2}{d\tau} = -k_2\Lambda'^2 \qquad (\leq 0) \tag{28}$$

The time derivative of the mission function is negative semidefinite, as shown in Eq. (28). Through use of Eqs. (26) and (27), the tension $\hat{T}_2$ provides the control algorithm for the tethered system and is applied to the in-plane and the out-of-plane motions [Eqs. (1)] after the time period t_f.

V. Numerical Results for Control Through Optimal Path

The deployment phase is studied for present optimal control numerically with the initial conditions disturbed slightly from the optimal path:

$$l = 1.1 \text{ km}, \qquad l' = 10 \text{ m/s}, \qquad \Theta = 0.1, \qquad \Theta' = 0$$
$$\phi = 0.1, \qquad \phi' = 0 \qquad \text{at} \qquad t = 0 \tag{29a}$$

and with the terminal state variables

$$l_m = 100 \text{ km}, \qquad l_m' = \Theta_m = \Theta_m' = \phi_m = \phi_m' = 0 \quad \text{at} \quad t = t_f \tag{29b}$$

Furthermore, errors with order of ±1.0% are included in the numerical simulation as unavoidable state uncertainty.

Figures 5a and 5b show the time histories of the subsatellite position in the in plane and out of plane during the deployment with $a_1 = 12.98$, $b_1 = 1.000$, $k_1 = 6.37 \times 10^2$, and $c_1 = 0.001$. The dotted line represents the optimal path for the tethered subsatellite. The dashed line represents a trajectory when the optimal control input $\hat{T}_t$ without any feed back is applied and the solid line represents a trajectory when the control tension $\hat{T}_1$ is applied by the tracking control. The deviation from the optimal path apparently increases

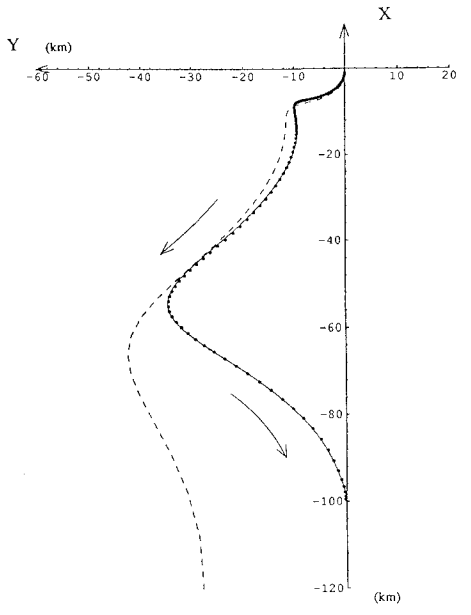

Fig. 5a In-plane motion of tethered subsatellite for deployment phase. ··· —optimal path for the tethered subsatellite; - - - —trajectory under the optimal control tension with slight initial deviation; —— — trajectory under the tracking-type control with slight initial deviation; (Initial conditions: $l = 1.1$ km, $l' = 10$ m/s, $\Theta = 0.1$, $\Theta' = 0.0$, $\phi = 0.1$, $\phi' = 0.0$).

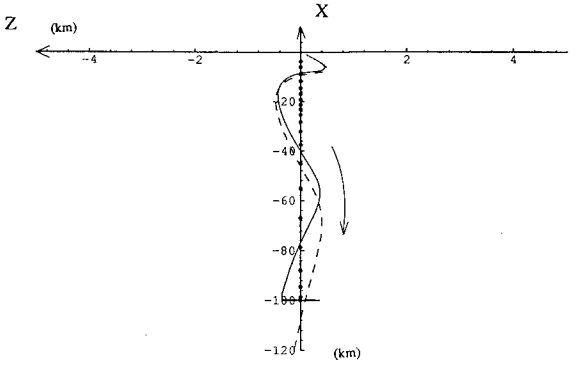

Fig. 5b Out-of-plane motion of tethered subsatellite for deployment phase. ··· —optimal path for the tethered subsatellite; - - - —trajectory under the optimal control tension with slight initial deviation; —— — trajectory under the tracking-type control with slight initial deviation; (Initial conditions: $l = 1.1$ km, $l' = 10$ m/s, $\Theta = 0.1$, $\Theta' = 0.0$, $\phi = 0.1$, $\phi' = 0.0$).

for the case of the control inputs $\hat{T}_t$ (dashed line). The reason is easily recognized by investigating Fig. 5c, which shows the time history of the multiplier functions $\lambda(t)$. The components of $\lambda(t)$ are defined as

$$\frac{\partial J}{\partial x} = \lambda(t) \tag{30}$$

and this equation means that the multiplier functions are the gradient of the performance index with respect to the state vector. If the initial absolute value of the multiplier is large, as shown in Fig. 5c, even slight deviation in the initial condition consequently causes the trajectory for the optimal control $\hat{T}_t$ to deviate from the optimal path. In other words, it is not easy to keep the optimal conditions when the gradient of the performance index with respect to the state variables becomes large. It is seen from Fig. 5a that the optimal path is traced very well by the trajectory obtained with the control tension $\hat{T}_1$ of the tracking type compared with the trajectory obtained with the neighboring optimum feedback control under the same deviation of the initial conditions shown in Fig. 3. The tension control is changed

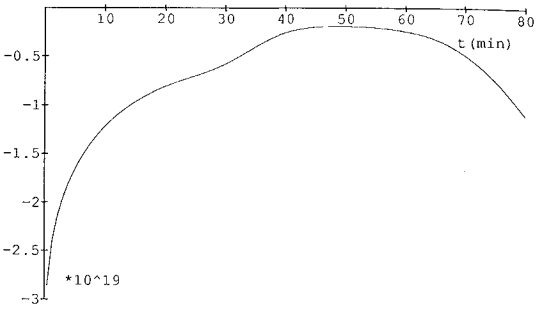

Fig. 5c Variation of multipliers function with respect to nondimensional length.

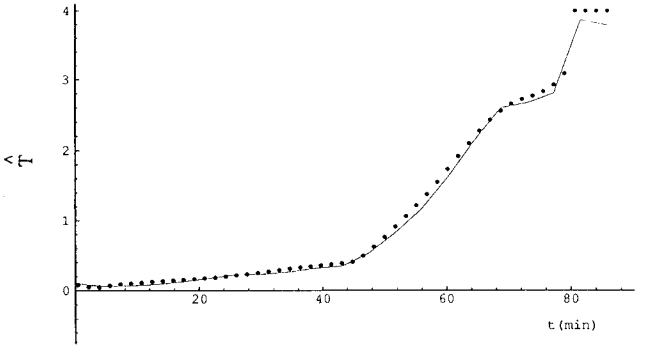

Fig. 5d Variation of nondimensional tension; ··· —optimal control tension of the optimal path; —— —control tension which is obtained from the Mission-Function control.

to $\hat{T}_2$ after the optimal path is completed at t_f (83 min). It amounts to about 350 min for the state variables to converge into an objective state [Eq. (29b)] in this case of the deployment phase.

Results of the numerical simulation for the retrieval case are shown in Figs. 6a–6c. The initial conditions and the terminal conditions are selected as follows:

$$\begin{aligned} l = 101 \text{ km}, \qquad \Theta = 0.01, \qquad \phi = 0.001 \\ l' = \Theta' = \phi' = 0 \qquad \text{at} \qquad t = 0 \end{aligned} \tag{31a}$$

$$\begin{aligned} l_m = 1 \text{ km}, \qquad l'_m = \Theta_m = \Theta'_m = \phi_m = \phi'_m = 0 \\ \text{at} \qquad t = t_f \end{aligned} \tag{31b}$$

The time histories of the subsatellite in the in plane and the out of plane during retrieval are shown in Figs. 6a and 6b in the same manner as in Figs. 5a and 5b. In this case, the values of the positive weighting coefficients are set to be $a_1 = 5.10$, $b_1 = 1.000$, $k_1 = 2.12 \times 10^4$, and $c_1 = 0.001$. It is obviously seen from these results that the present tracking control works very well. Figure 6c shows the time responses of Θ and ϕ . The out-of-plane motion is stabilized by the tension control that is led from the mission function [Eqs. (26)], similar to the deployment phase, even if the tension does not include the angle and its rate in the out of plane. The reason is that the out-of-plane motion is reduced to the undamped motion by suppressing the in-plane motion Λ and Θ [Eqs. (1c)]. The tension control is changed to $\hat{T}_2$ after the optimal path is completed at t_f (70 min). It amounts to about 500 min for the state variables to converge into an objective state [Eq. (31b)]. Figure 6e shows that the mission function decreases as time increases.

Comparing the optimal paths with the case of terminal time fixed (Figs. 2a and 2b) and those with the case of terminal time unspecified (Figs. 5a and 6a), it is seen that the maximum displacement of the subsatellite from the X axis is reduced due to the process of optimization on the unspecified terminal time. It is concluded that the optimization of the terminal time is important to obtain the

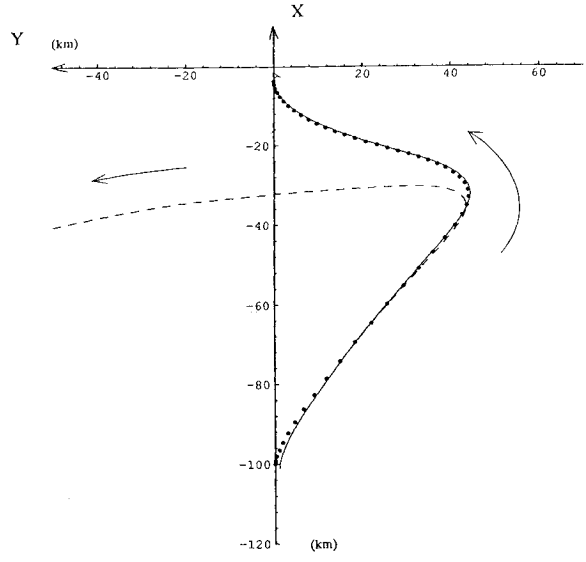

Fig. 6a In-plane motion of tethered subsatellite for retrieval phase; · · · —optimal path for the tethered subsatellite; - - - —trajectory under the optimal control tension with slight initial deviation; —— —trajectory under the tracking-type control with slight initial deviation; (Initial conditions: $l = 101$ km, $l' = 0.0$ m/s, $\Theta = 0.01$, $\Theta' = 0.0$, $\phi = 0.001$, $\phi' = 0.0$).

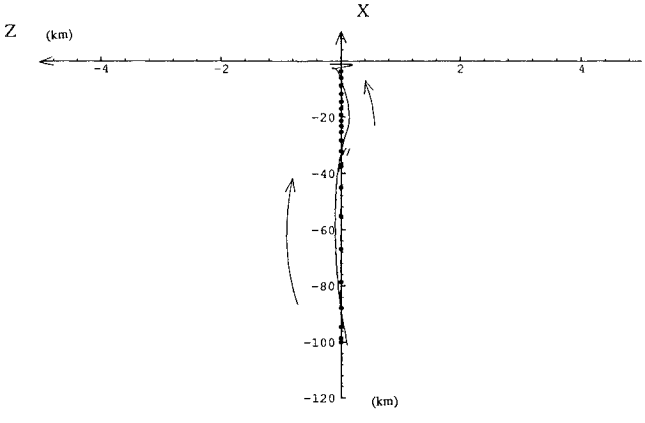

Fig. 6b Out-of-plane motion of the tethered subsatellite for retrieval phase; · · · —optimal path for the tethered subsatellite; - - - —trajectory under the optimal control tension with slight initial deviation; —— — trajectory under the tracking-type control with slight initial deviation; (Initial conditions: $l = 101$ km, $l' = 0.0$ m/s, $\Theta = 0.01$, $\Theta' = 0.0$, $\phi = 0.001$, $\phi' = 0.0$).

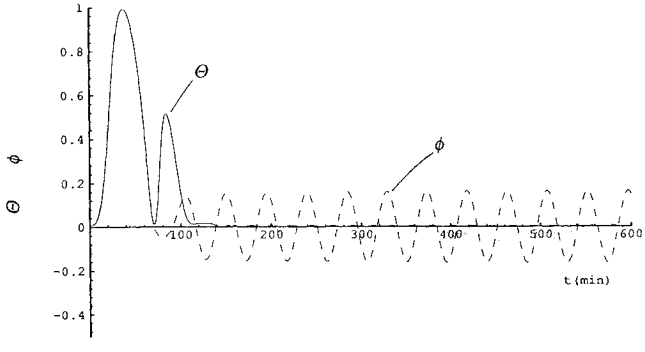

Fig. 6c Variation of position angle in the in-plane and out-of-plane motion; —— —position angle in the in-plane motion; - - - —position angle in the out-of-plane motion.

optimal path for the deployment/retrieval phase. The value of the nondimensional length Λ on the optimal path for the retrieval case does not converge into the objective state equation (3) due to sensitivity of the conditions on the object state equation (3) for solving this two-point boundary-value problem with inequality constraints on tether tension as in Eq. (6).

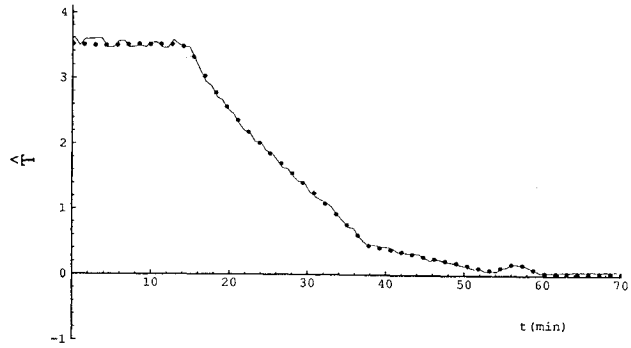

Fig. 6d Variation of the nondimensional tension; · · · —optimal control tension, of the optimal path; —— —control tension, which is obtained from the Mission-Function control.

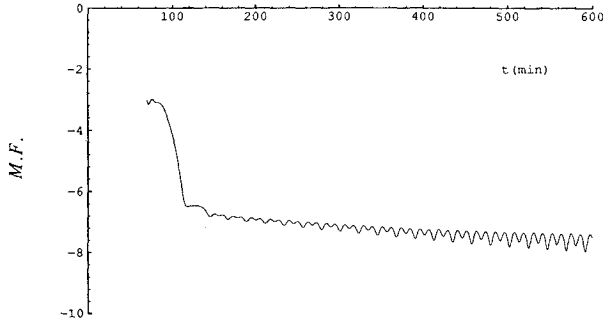

Fig. 6e Plot on a log scale of mission function against time.

VI. Conclusions

The control problem of the deployment/retrieval of the tethered subsatellite has been studied through the application of the mission-function control and optimal control. Results of numerical simulation show that, if the initial conditions deviate slightly from the initial conditions of the optimal path, a preferable control performance cannot be obtained by either the optimal control tension only or the tension including the neighboring optimum feedback control. The trajectory under the tracking-type control using the mission-function control converges into the objective state in the in-plane motion; therefore, the out-of-plane motion is stabilized under the existence of error in sensor measurement and the deviation of the state variable from the optimal path. It is concluded that the present control algorithm assures excellent performance for the control of the deployment/retrieval of the tethered subsatellite.

References

[1]Bekey, I., "Tethers Open New Space Options," *Astronautics and Aeronautics*, Vol. 21, No. 4, April 1983, pp. 33–40.

[2]Wood, G. M., Siemers, P. M., Squires, R. K., Wolf, H., Carlomagno, G. M., and Luca, L., "Downward-Deployed Tethered Platforms for High-Enthalpy Aerothermodynamic Research," *Journal of Spacecraft and Rockets*, Vol. 27, No. 2, 1990, pp. 216–221.

[3]Brown, K. G., Melfi, L. T., Jr., Upchurch, B. T., and Wood, G. M., Jr., "Downward-Deployed Tethered Satellite Systems, Measurement Techniques, and Instrumentation: A Review," *Journal of Spacecraft and Rockets*, Vol. 29, No. 5, 1992, pp. 671–677.

[4]Stuart, D. G., "Guidance and Control for Cooperative Tether-Mediated Orbital Rendezvous," *Journal of Guidance, Control, and Dynamics*, Vol. 13, No. 6, 1990, pp. 1102–1108.

[5]Bainum, P. M., Diarra, C. M., and Kumar, V. K., "Shuttle-Tethered Subsatellite System Stability with a Flexible Massive Tether," *Journal of Guidance, Control, and Dynamics*, Vol. 8, No. 2, 1985, pp. 230–234.

[6]De Matteis, G., and de Socio, L. M., "Dynamics of a Tethered Satellite Subjected to Aerodynamic Force," *Journal of Guidance, Control, and Dynamics*, Vol. 14, No. 6, 1991, pp. 1129–1135.

[7]Misra, A. K., and Modi, V. J., "Dynamics and Control of Tether Connected Two-Body Systems —A Brief Review," IAF-82-315, *33rd Congress of the International Astronautical Federation*, France, 1982, pp. 473–514.

[8]Misra, A. K., and Modi, V. J., "A Survey on the Dynamics and Control of Tethered Satellite Systems," *Tethers in Space, Advances in the Astronautical*

Sciences, Vol. 62, 1987, pp. 67–720.

[9]Misra, A. K., and Modi, V. J., "Dynamics of a Tether Connected Payload Deploying from the Space Shuttle," *Second Virginia Polytechnic Inst. and State Univ./AIAA Symposium on Dynamics and Control of Large Flexible Spacecraft* (Blacksburg, VA), June 1979, pp. 21–23.

[10]Modi, V. J., Chang-fu, G., and Misra, A. K., "Effect of Damping on the Control Dynamics of the Space Shuttle Based Tethered Systems," *Journal of the Astronautical Sciences*, Vol. 16, No. 1, 1983, pp. 135–149.

[11]Xu, D. M., and Misra, A. K., "Thruster-Augmented Active Control of a Tethered Subsatellite System During Its Retrieval," *Journal of Guidance, Control, and Dynamics*, Vol. 9, No. 6, 1986, pp. 663–672.

[12]Liangdong, L., and Bainum, P. M., "Effect of Tether Flexibility on the Tethered Shuttle Subsatellite Stability and Control," *Journal of Guidance, Control, and Dynamics*, Vol. 12, No. 6, 1989, pp. 866–873.

[13]Banerjee, A. K., "Dynamics of Tethered Payloads with Deployment Rate Control," *Journal of Guidance, Control, and Dynamics*, Vol. 13, No. 4, 1990, pp. 759–762.

[14]No, T. S., and Cochran, J. E., Jr., "Dynamics and Control of a Tethered Flight Vehicle," AAS/AIAA Astrodynamics Specialist Conference, Durango, CO, Aug. 1991.

[15]Kim, E., and Vadali, S. R., " Nonlinear Feedback Deployment and Retrieval of Tethered Satellite Systems," *Journal of Guidance, Control, and Dynamics*, Vol. 15, No. 1, 1992, pp. 28–34.

[16]Rupp, C. C., "A Tether Tension Control Law for Tethered Satellite Deployment Along the Local Vertical," NASA TM X-64963, 1975.

[17]Bainum, P. M., Kumar, V. K., "Optimal Control of the Shuttle-Tethered-Subsatellite System," *Acta Astronautica*, Vol. 7, 1980, pp. 1333–1348.

[18]Fujii, H., and Ishijima, S., "Mission Function Control for Deployment and Retrieval of a Subsatellite," *Journal of Guidance , Control, and Dynamics*, Vol. 12, No. 2, 1989, pp. 243–247.

[19]Fujii, H., Uchiyama, K., and Kokubun, K., "Mission Function Control of Deployment/Retrieval of Tethered Subsatellite: In-Plane and Out-of-Plane Motion," *Journal of Guidance, Control, and Dynamics*, Vol. 14, No. 2, 1991, pp. 471–473.

[20]Fujii, H., Uchiyama, K., and Kokubun, K., "Application of the Mission Function Control to Deployment/Retrieval of a Subsatellite," *Proceedings of the Sixteenth International Symposium on Space Technology and Science*, Sapporo, Japan, 1988, p. 349.

[21]Junkins, J. L., Rahman, Z. H., and Bang, H., "Near-Minimum Time Control of Distributed Parameter Systems: Analytical and Experimental Results," *Journal of Guidance, Control, and Dynamics*, Vol. 14, No. 2, 1991, pp. 406–415.

[22]Lasdon, L. S., Mitter, S. K., and Waren, A. D., "The Conjugate Gradient Method for Optimal Control Problems," *IEEE Transactions on Automatic Control*, Vol. AC-12, No. 2, 1967, pp. 132–138.

[23]Quintana, V. H., and Davison, E. J., "Clipping-off Gradient Algorithm to Compute Optimal Controls with Constrained Magnitude," *International Journal of Control*, Vol. 20, No. 2, 1974, pp. 243–255.

[24]Bryson, E., Jr., and Ho, Y.-C., *Applied Optimal Control—Optimization, Estimation and Control*, Hemisphere, New York, 1975.